Acta Pharmacologica Sinica

www.nature.com/aps

ARTICLE

Carnosine suppresses human glioma cells under normoxic and hypoxic conditions partly via inhibiting glutamine metabolism

Yu-jia Fang[1], Ming Wu[1], Hai-ni Chen[1], Tian-tian Wen[1], Jian-xin Lyu[1,2] and Yao Shen[1]

L-Carnosine (β-alanyl-*L*-histidine) is a naturally occurring dipeptide, which has shown broad-spectrum anticancer activity. But the anticancer mechanisms and regulators remain unknown. In this study, we investigated the effects of carnosine on human glioma U87 and U251 cell lines under normoxia (21% O_2) and hypoxia (1% O_2). We showed that carnosine (25−75 mM) dose-dependently inhibited the proliferation of the glioma cells; carnosine (50 mM) inhibited their colony formation, migration, and invasion capacity. But there was no significant difference in the inhibitory effects of carnosine under normoxia and hypoxia. Treatment with carnosine (50 mM) significantly decreased the expression of glutamine synthetase (GS) at the translation level rather than the transcription level in U87 and U251 cells, both under normoxia and hypoxia. Furthermore, the silencing of GS gene with shRNA and glutamine (Gln) deprivation significantly suppressed the growth, migratory, and invasive potential of the glioma cells. The inhibitory effect of carnosine on U87 and U251 cells was partly achieved by inhibiting the Gln metabolism pathway. Carnosine reduced the expression of GS in U87 and U251 cells by promoting the degradation of GS through the proteasome pathway, shortening the protein half-life, and reducing its stability. Given that targeting tumor metabolism is a proven efficient therapeutic tactic, our results may present new treatment strategies and drugs for improving the prognosis of gliomas.

Keywords: glioma; hypoxia; carnosine; glutamine synthetase; proteasome; tumor metabolism

Acta Pharmacologica Sinica (2021) 42:767–779; https://doi.org/10.1038/s41401-020-0488-1

INTRODUCTION

Gliomas, including astrocytoma, oligodendroglioma, and ependymoma, are tumors of neuroectoderm origin caused by glial cells or precursor cells [1]. Glioma is the most common type of malignant brain tumor, accounting for 81% of malignant brain tumors, and the most lethal primary brain tumor [2, 3]. Its prognosis is poor because of the limited amount of tumor tissue that can be safely removed, resistance of the residual tumor to radiotherapy and chemotherapy after operation, and blood–brain barrier, a challenge for drug delivery [4]. Glioma stem cells are another very important feature of glioma. Glioma stem cells have strong DNA-repair mechanisms, leading to chemoradiotherapy resistance [5], and the ability to differentiate into stroma and vascular structures that support tumor growth [6]. The need to find effective treatment methods and drugs for glioma is urgent.

Tumor hypoxia can strongly induce cells to develop aggressive and refractory phenotypes, leading to rapid progress and poor prognosis [7]. Hypoxia is a hallmark of gliomas, which, therefore, histologically show the pathological characteristics of pseudopalisading necrosis and vascular hyperplasia [8]. On the other hand, a growing number of studies have found that mitochondrial function in tumor cells is not absent but rather suppressed. Under some conditions, the metabolic activity of mitochondria in tumor cells is activated to promote the rapid growth of tumor cells [9–11]. Both the glycolysis and mitochondrial oxidative phosphorylation pathways play important roles in tumor cell proliferation and/or metastasis. Therefore, the need to find new tumor treatment strategies and drugs that can simultaneously target the glycolysis pathway and mitochondrial aerobic respiratory pathway is substantial.

Glutamine (Gln) was shown to play an important role in cell proliferation in the 1950s [12]. Gln synthesis is upregulated in some cancers; for example, some human gliomas accumulate large amounts of Gln by synthesizing glucose-derived carbon under the catalysis of glutamine synthesis (GS) [13]. This promotes the de novo synthesis of purines and the biosynthesis of some essential amino acids, making glioma cells self-sufficient in meeting the need for Gln. Consistent with this metabolic phenotype, GS is expressed in most gliomas [14]. Research has shown that when primary glioblastoma cells maintain a stem cell-like state, GS expression is significantly increased, and glutamate (Glu) is taken up rather than released, rendering the growth of glioblastoma-like cells independent of extracellular Gln [14].

Carnosine is a naturally occurring dipeptide composed of β-alanine and *L*-histidine [15]. In vivo and in vitro experiments have shown that carnosine is a powerful antioxidant [16], free radical scavenger [17], and effective antiglycation agent [18]. In addition, carnosine is well tolerated in humans, has no known drug interactions or serious adverse reactions, and can freely pass through the blood–brain barrier [19]. In recent years, the broad-spectrum antitumor effect of carnosine has attracted the attention of researchers [20, 21]. In our previous studies on gastric cancer, we found that the antitumor effect of carnosine may be achieved

[1]Key Laboratory of Laboratory Medicine, Ministry of Education, School of Laboratory Medicine and Life sciences, Wenzhou Medical University, Wenzhou 325035, China and [2]Zhejiang Provincial People's Hospital, Affiliated People's Hospital of Hangzhou Medical College, Hangzhou 310014, China
Correspondence: Yao Shen (yueshen-2002@163.com)

Received: 24 March 2020 Accepted: 19 July 2020
Published online: 11 August 2020

by inhibiting both glycolysis and mitochondrial aerobic respiration [10, 22]. However, it is not clear whether carnosine inhibits the proliferation, migration, and invasion of glioma cells by inhibiting glycolysis, mitochondrial aerobic metabolism, or both.

Therefore, in this study, we explored the effects of carnosine on the proliferation, migration, and invasion of glioma cells (U87 and U251 cells) under conditions of normoxia and hypoxia (1% O_2), and explored its potential molecular mechanism.

MATERIALS AND METHODS

Reagents

L-Carnosine was purchased from Sigma (St. Louis, MO, USA). Cycloheximide (CHX), chloroquine diphosphate (CLQ), and MG132 were purchased from MedChemExpress (Shanghai, China). A trypsin-EDTA solution, BCA protein concentration detection kit, 3-(4,5-dimethyl-2-thiazolyl)-2,5-diphenyl-2-H-tetrazolium bromide (MTT) powder, immunostaining fixative, and TRIzol reagent were purchased from Beyotime Institute of Biotechnology (Nanjing, China). Fetal bovine serum (FBS), high-glucose Dulbecco's modified Eagle's medium (DMEM), and Gln-free DMEM were obtained from GIBCO-BRL (Grand Island, NY, USA). The PrimeScript™ RT reagent kit and TB Green®*Premix Ex Taq*™ II were obtained from TakaRa Biotechnology Co., Ltd. (Dalian, China). An Annexin V-APC/PI apoptosis detection kit was from KeyGenBiotech (Jiangsu, China).

Cell culture and drug treatment

The U87 human glioma cell line was purchased from the Institute of Cell Biology, Chinese Academy of Sciences (Shanghai). The U251 cell line was purchased from the China Center for Type Culture Collection (CCTCC, Wuhan). Primary cultured rat cortical astrocytes were obtained through protocols described in our previously published article [23]. The cells were cultured in DMEM (containing 4 mM Gln; the DMEM was used within 2 weeks to avoid Gln degradation) supplemented with 10% FBS, 100 U/mL penicillin G, and 100 μg/mL streptomycin. Some cells were cultured at 37 °C in 5% CO_2 and 21% O_2 in a humidified incubator (Thermo Fisher Scientific, MA, USA) under normoxic conditions. Other cells were cultured at 37 °C in 5% CO_2 and 1% O_2 in a humidified incubator (Galaxy 170R incubator, Eppendorf, Germany) under hypoxic conditions. Testing showed that the hypoxia performance of the tri-gas incubator was normal (Supplementary Fig. 1). Cells in logarithmic growth phase were digested with trypsin at a ratio of 1:3. The subcultured cells were seeded onto 96- or 6-well plates at a density of 5×10^3 or 1×10^6 cells/well. For drug treatments, 24 h after the cells were plated, they were treated with carnosine at different concentrations (25 mM, 50 mM, and 75 mM) for different intervals (24 h, 48 h, and 72 h). To deplete Gln, cells were cultured in Gln-free DMEM.

Cell viability assay

Cell viability (mitochondrial activity) was detected by the MTT reduction assay. Cells were seeded onto 96-well plates at a density of 5×10^3 cells/well with three wells used for each group. At the end of the experiment, the medium was discarded, and the cells were then incubated with 0.5 mg/mL MTT in a cell incubator for 4 h. Then, the supernatant was discarded, and 100 μL of DMSO was added to every well. After the crystal violet solution had completely dissolved, MTT metabolism was quantitated spectrophotometrically at 570 nm in a multimode microplate reader (Thermo Fisher Scientific, MA, USA). The results are described as the percentage of MTT reduction, with the absorbance of the control group set at 100%.

Colony-formation assay

Cells were seeded into six-well plates at a density of 250–300 cells per well with three wells used for each group and then treated with carnosine (50 mM). The cells were cultured for 14 days in DMEM supplemented with 1% FBS, 100 U/mL penicillin G, and 100 μg/mL streptomycin, and the medium was changed every 3 or 4 days. Finally, the cells were fixed with immunostaining fixative and stained with a solution of crystal violet dye.

Wound-healing assay

U87 and U251 cells were plated in 6-well plates at a density of 90%. The cells were scratched with a sterile 10-μL pipette tip. Then, the cells were washed with PBS to remove floating cellular debris. The cells were then cultured in DMEM supplemented with 1% FBS and carnosine (50 mM). Every 12 h, the wounds were photographed, and the wound-closure rate was assessed by the following formula: wound-closure rate (%) $= (W_0 - W_t/W_0) \times 100\%$, where W_0 is the wound width at 0 h and W_t is the wound width at a given time point (12–24 h).

Cell migration and invasion assays

Cell invasion assays were carried out using BD BioCoatMatrigel Invasion Chambers (24-well insert, 8-μm pore size, BD Biosciences, Bedford, MA) following the manufacturer's instructions. U87 and U251 cells were trypsinized, resuspended in serum-free DMEM, and transferred to the upper chamber of Transwell inserts (5×10^4 cells/well). DMEM including 20% FBS was added to the lower chamber. Cells were incubated for 24 h in a common cell incubator (21% O_2) or hypoxia incubator (1% O_2). Invasive cells were fixed with immunostaining fixative and stained with crystal violet dye. Noninvasive cells in the inner part of the chambers were removed with cotton swabs. The invaded cells in five random fields were photographed with a microscope. Each experiment was repeated three times. The cell migration assay was also performed with U87 cells and U251 cells with the procedure used for the invasion assay, except that the assay was performed without the Matrigel inserts.

Western blot analysis

When cells in a dish had grown to ~80%–90% confluency, they were treated with carnosine (50 mM), CHX (150 μg/mL), the proteasome inhibitor MG132 (5 μM), and the lysosome inhibitor CLQ (25 μM). After treatment, the medium was removed, and the cells were washed with PBS twice. Cells were lysed on ice with RIPA lysate containing PMSF for 10 min, followed by centrifugation at 14,000 × *g* for 30 min at 4 °C. The supernatant was harvested in a new Eppendorf tube, and the protein concentration was quantified via BCA protein concentration detection kit. Western blot analysis was performed by standard protocol. The following antibodies were used: mouse anti-tubulin (Beyotime Institute of Biotechnology, 1:1000), mouse anti-β-actin (Beyotime Institute of Biotechnology, 1:1000), rabbit anti-GS (Abcam, 1:2000), mouse anti-HIF-1α (Abcam, 1:2000), HRP-labeled goat anti-rabbit IgG (1:1000), and HRP-labeled goat anti-mouse IgG (1:2000, Beyotime Institute of Biotechnology, Nanjing, China).

Quantitative real-time polymerase chain reaction (qRT-PCR)

To determine gene expression, total RNA was isolated with TRIzol reagent according to the manufacturer's specifications, and purified RNA was quantified by spectrophotometry with a Nanodrop (Thermo Fisher Scientific, MA, USA). cDNA was synthesized from 1 μg of total RNA using the PrimeScript™ RT reagent kit according to the manufacturer's guidelines. qRT-PCR to amplify GS was performed using TB Green®*Premix Ex Taq*™ II with a CFX96 Real-Time PCR Detection System (Bio-Rad, CA, USA). The expression of β-actin was used as an internal control to normalize differences in individual samples compared with the control sample. Target gene expression (relative mRNA expression) was calculated by the $2^{-\Delta\Delta Ct}$ method, and is expressed as a fold change (mean ± SD) over the average β-actin expression, which was set at one. The qRT-PCR primers used for the experiment were

as follows: GS (Fw: 5′-TCATCTTGCATCGTGTGTGTG-3′; Rev: 5′-CTTCAGACCATTCTCCTCCCG-3′) and β-actin (Fw: 5′-CCCTGGCACCCAGCAC-3′; Rev: 5′-GCCGATCCACACGGAGTAC-3′).

Flow cytometry (FCM)
Cells were stained with Annexin V-APC and PI to evaluate apoptosis by flow cytometry according to the manufacturer's instructions (KeyGenBiotech, Jiangsu, China). Briefly, 1×10^6 trypsinized cells were washed with PBS and stained with 5 μL of PI and 5 μL of Annexin V-APC in 500 μL of 1 × binding buffer for 5 min at room temperature in the dark. Quantification of apoptotic cells was performed with a CytoFLEX (Beckman Coulter, CA, USA).

Gene silencing
Three different small-hairpin RNAs (shRNAs) targeting GS and a negative control (NC) sequence were inserted into the GV112 vector (GeneChem, Shanghai, China). After verification by gene sequencing, GV112-shLenti, the relevant NC plasmid, and two packaging plasmids (psPAX2 and pMD2.G, donated by Dr. Hongzhi Li, Wenzhou Medical University, Wenzhou, China) were transfected into 293T cells for 48 h using PolyJet (SignaGen, MD, USA). U87 and U251 cells were seeded in 60-mm dishes and cultured in DMEM for 24 h. Then, solution containing the virus was harvested, filtered, and used to infect the cell lines with polybrene (8 μg/mL). The expression level of GS in transfected cells was confirmed by real-time PCR and Western blotting. The cell line with the highest knockout efficiency was selected for follow-up experiments. The shRNA sequences used were as follows:

GS-shRNA, sense: 5′-CCAGGAGAAGAAGGGTTACTT-3′
NC, sense: 5′-TTCTCCGAACGTGTCACGT-3′

Statistical analysis
All data are presented as the mean ± SD of three or more independent experiments. Statistical analyses were conducted by SPSS 20.0. One-way ANOVA (analysis of variance) was applied for multiple comparisons, whereas comparisons between two groups were analyzed using Student's *t* test. $P < 0.05$ indicated statistical significance.

RESULTS

Effects of carnosine on the viability, colony-formation ability, and apoptosis of U87 and U251 cells cultured under normoxic and hypoxic conditions
We first examined the viability of U87 and U251 human glioma cells treated with carnosine at different concentrations (25, 50, and 75 mM) for different durations (24, 48, and 72 h) under normoxic and hypoxic conditions. This concentration gradient was chosen because Holliday and McFarland demonstrated that HFF-1 cells derived from human foreskin grew well in medium containing 50 mM carnosine [24]. Interestingly, the different oxygen concentrations had similar effects on both cell lines. Carnosine treatment significantly decreased cell viability in a concentration- and time-dependent manner. Under normoxic conditions, the cell viability of U87 and U251 cells treated with 25 and 50 mM carnosine for 48 and 72 h decreased to 85.49% and 38.33%, respectively, and 76.78% and 45.99%, respectively. Under hypoxic conditions, the cell viability of U87 and U251 cells treated with 25 and 50 mM carnosine for 48 and 72 h decreased to 92.44% and 51.4% and 84.05% and 53.69%, respectively (Fig. 1a).

In the colony-formation assay, the formation of colonies from U87 cells treated with carnosine under normoxia and hypoxia was inhibited by 83.97% and 87.36%, respectively, and that from U251 cells was inhibited by 85.30% and 83.57%, respectively (Fig. 1b). Flow cytometry analysis of apoptosis showed that carnosine did change the level of apoptosis in U87 or U251 cells, under either normoxic or hypoxic conditions (Fig. 1c). These data demonstrated that carnosine has a significant inhibitory effect on the proliferation of human glioma cells. There were no differences in the inhibitory effect of carnosine on cell viability and cell proliferation between normoxic and hypoxic conditions.

Carnosine suppressed glioma cell migration and invasion under normoxia and hypoxia
In the wound-healing assay, for both U87 and U251 cells, the wound-closure rate in the carnosine-treatment group was significantly lower than that in the control group under different oxygen conditions (U87 cells: normoxia: 46.93%, normoxia + Car: 33.04%, $P < 0.05$; hypoxia: 36.14%, hypoxia + Car: 21.69%, $P < 0.01$; U251 cells: normoxia: 46.26%, normoxia + Car: 36.81%, $P < 0.05$; hypoxia: 37.41%, hypoxia + Car: 21.67%, $P < 0.01$, Fig. 2a).

Transwell migration assays showed that the number of cells that passed through the membrane of chambers seeded with cells treated with 50 mM carnosine was significantly lower than that with cells that did not undergo carnosine treatment under both normoxia and hypoxia. Under normoxic conditions, the migration of U87 and U251 cells treated with carnosine decreased by 47.92% and 57.49%, respectively. Under hypoxic conditions, the migration of U87 and U251 cells treated with carnosine decreased by 58.19% and 53.47%, respectively (Fig. 2b). Data obtained from cell invasion assays also showed that the number of invaded cells in the carnosine group was much less than that in the control group for both U87 and U251 cells under both normoxia and hypoxia (43.13% and 63.62% decrease in U87 and U251 cells, respectively, under normoxia; 61.03% and 49.69% decrease in U87 and U251 cells, respectively, under hypoxia; $P < 0.01$, Fig. 2b). Taken together, these results show that carnosine decreased the migration and invasion of U87 and U251 cells under both normoxic and hypoxic conditions, and that the inhibitory effects of carnosine under normoxic and hypoxic conditions did not differ.

Effects of carnosine on GS protein and mRNA levels in U87 and U251 cells under normoxic and hypoxic conditions
Gln was shown to play an important role in cell proliferation as early as the 1950s [12]. The enzyme GS catalyzes the de novo synthesis of Gln. GS is expressed in most human glioblastoma cells, and its expression is associated with poor prognosis [25]. Therefore, we first examined the effect of 50 mM carnosine on the protein expression of GS in two cell lines under normoxic and hypoxic conditions. Under normoxic conditions, carnosine inhibited GS protein expression in U87 and U251 cells by 45% and 41%, respectively; under hypoxia, carnosine inhibited GS protein expression in U87 and U251 cells by 47% and 37%, respectively (Fig. 3a). The above data showed that carnosine significantly inhibited the protein expression of GS in U87 and U251 cells, and that the inhibition rates under normoxic and hypoxic conditions did not differ. We speculated that carnosine may have affected the expression of GS at the transcription level and verified this hypothesis by real-time PCR experiments. The results showed that carnosine did not affect the mRNA level of GS in U87 or U251 cells (Fig. 3b). Carnosine reduced the protein expression of GS, but did not affect the mRNA level of GS, that is, carnosine did not affect the expression of GS at the transcription level.

Effects of carnosine and Gln deprivation on GS protein expression in U87 and U251 cells under normoxic and hypoxic conditions
The antitumor effect of carnosine is thought to be exerted through multiple targets [26]. To investigate whether the observed decrease in GS protein expression was indeed caused by carnosine, we first treated U87 and U251 cells with 50 mM carnosine for different durations (24 and 48 h), and then treated different groups of U87 and U251 cells with carnosine at different concentrations (25, 50, and 75 mM) for 48 h. The cellular proteins were extracted, and we detected the effects of normoxia, hypoxia, Gln (4 mM) treatment, and Gln deprivation on GS protein

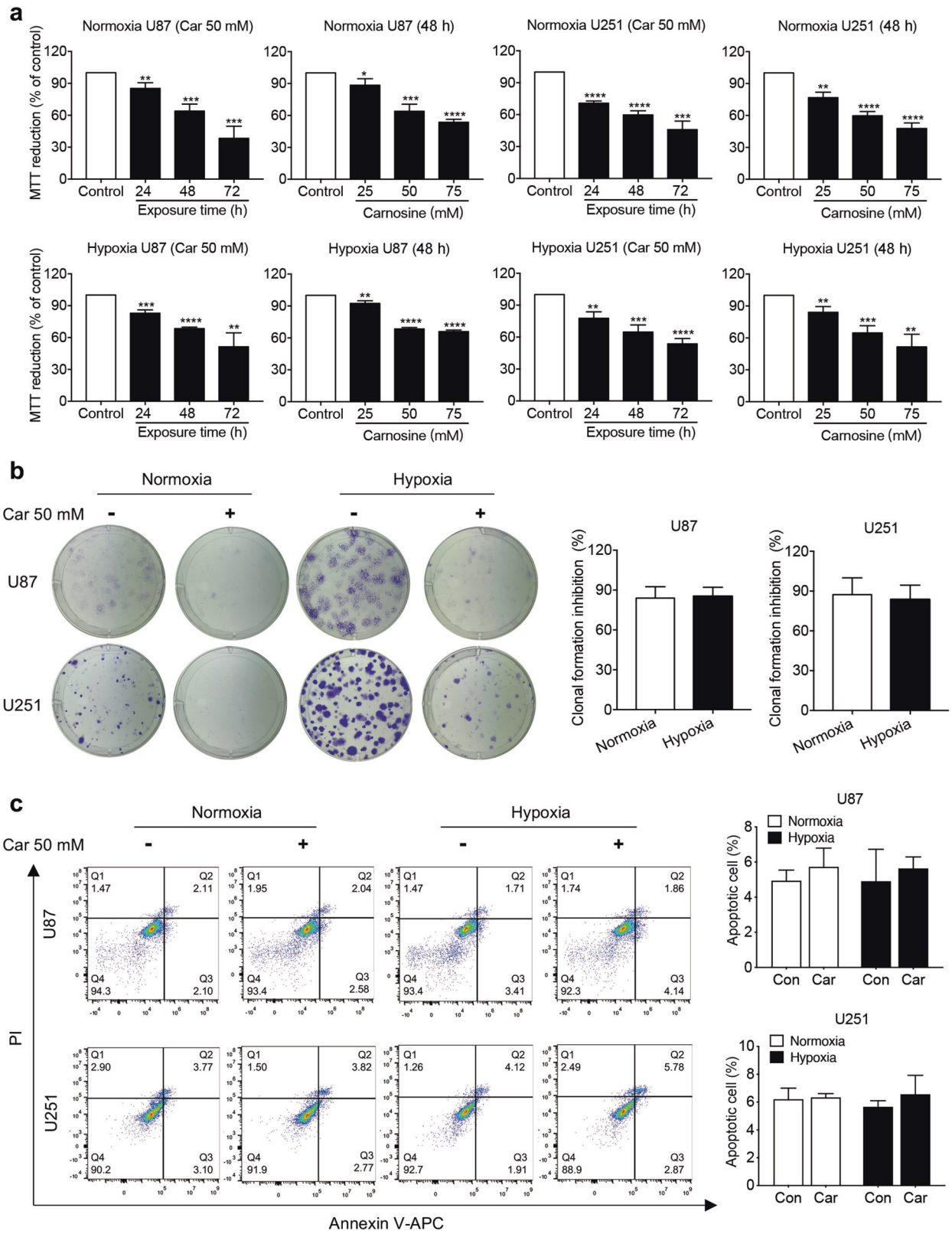

Fig. 1 Effects of carnosine on the viability, colony formation, and apoptosis of U87 and U251 cells cultured under normoxic and hypoxic conditions. **a** U87 and U251 cells were exposed to carnosine at different conditions (25, 50, and 75 mM) for 48 h, or 50 mM carnosine for different time periods (24, 48, and 72 h). Cell viability was determined by MTT assay. **b** Colony formation of cells treated with 50 mM carnosine for 14 days under normoxic and hypoxic conditions was assessed. Clone-formation inhibition rate = (a−b)/a × 100%, where a = number of clones under normoxia or hypoxia without carnosine treatment and b = number of clones under normoxia or hypoxia with carnosine treatment. **c** Under normoxic and hypoxic conditions, cells were treated with 50 mM carnosine for 48 h, after which flow cytometry was used to detect the apoptosis level. Data are expressed as the mean ± SD. $n = 3$. *$P < 0.05$, **$P < 0.01$, ***$P < 0.001$, ****$P < 0.0001$ vs. the control group or normoxia group.

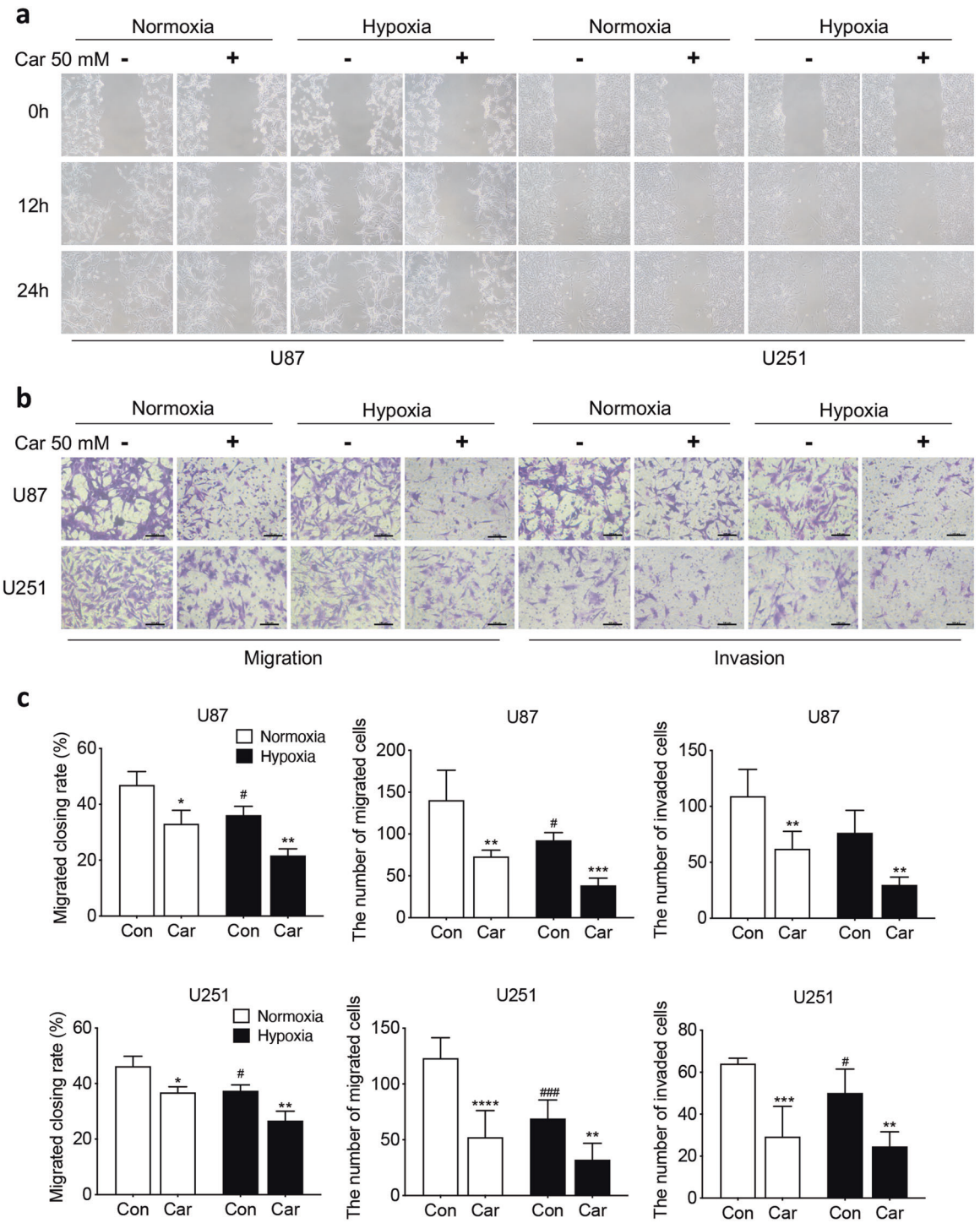

Fig. 2 Carnosine inhibited U87 and U251 cell migration and invasion under normoxia and hypoxia. Scratch assays (**a**, 100×) and Transwell migration assays (**a**) were used to explore the effect of carnosine on the migration capacity of U87 and U251 cells. **b** Transwell invasion assays were used to evaluate whether carnosine could also influence the invasion of U87 and U251 cells. **c** Quantitative analysis of the wound-closure rate in the wound-healing assay and number of migrated and invaded cells was conducted by Transwell assay. Car stands for carnosine. The results are expressed as the mean ± SD. $n \geq 3$. Scale bar = 100 μm. $^{*}P < 0.05$, $^{**}P < 0.01$, $^{***}P < 0.001$, $^{****}P < 0.0001$ vs. the control group. $^{\#}P < 0.05$, $^{\#\#\#}P < 0.001$ vs. the normoxia group.

expression. Regardless of the conditions, the inhibitory effect of carnosine on GS expression was time- and concentration-dependent (Fig. 4). The inhibitory rates of 50 mM carnosine treatment for 48 h on the expression of GS protein in U87 cells under conditions of normoxia and 4.0 mM Gln treatment, normoxia and Gln deprivation, hypoxia and 4.0 mM Gln treatment, and hypoxia and Gln deprivation were 60%, 47%, 61%, and 66%, respectively, and in U251 cells, the corresponding inhibitory rates were 56%, 50%, 51%, and 38%, respectively. Under conditions of normoxia and 4.0 mM Gln treatment, normoxia and Gln deprivation, hypoxia and 4.0 mM Gln treatment, and hypoxia and Gln deprivation, the inhibitory rates of 75 mM carnosine treatment for

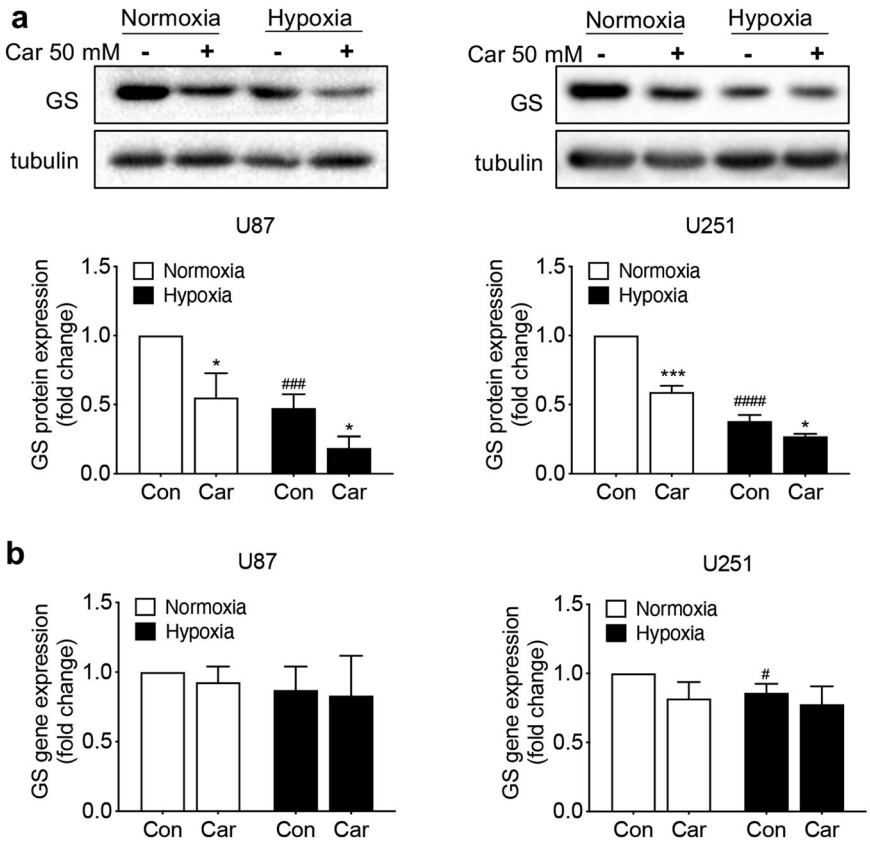

Fig. 3 Carnosine downregulated GS at only the protein expression but did not affect its RNA expression. a Western blot analysis of GS protein levels in cultured U87 and U251 cells treated with carnosine for 48 h under normoxic and hypoxic conditions. **b** Real-time PCR analysis of the GS mRNA level in cultured U87 and U251 cells treated with carnosine for 48 h under normoxic and hypoxic conditions. The results are expressed as the mean ± SD. $n = 3$. $^{*}P < 0.05$, $^{***}P < 0.001$ vs. the control group. $^{\#}P < 0.05$, $^{\#\#\#}P < 0.001$, $^{\#\#\#\#}P < 0.0001$ vs. the normoxia group.

48 h on the expression of GS protein in U87 cells were 82%, 54%, 81%, and 75%, respectively, and the corresponding rates in U251 cells were 80%, 65%, 87%, and 45%, respectively. The above data indicate that the observed decrease in GS protein expression was indeed caused by carnosine.

Carnosine combined with Gln deprivation enhanced cell growth inhibition and induced apoptosis in U87 and U251 cells under normoxic and hypoxic conditions

To further determine whether U87 and U251 cells are dependent on exogenous Gln, and whether exogenous Gln would affect the inhibitory effect of carnosine on glioma cell proliferation, we performed MTT assays. Under normoxic and hypoxic conditions, U87 and U251 cells were deprived of Gln for 24, 48, and 72 h, after which MTT assays were carried out to detect changes in cell viability. Gln deprivation inhibited the activity of U87 cells by ~20%–30%, but it had a greater influence on U251 cells. With increasing duration, the highest inhibitory effect of Gln deprivation on U251 cells was a 69% decrease (72 h under hypoxia) (Fig. 5a, b). The U251 cells were clearly more sensitive to the loss of exogenous Gln than U87 cells. The two glioma cell lines, both of which expressed GS, showed such differences after exogenous Gln deprivation, which inspired our hypothesis. To explore whether the expression of GS in the two cell lines changed with exogenous Gln deprivation, we carried out Western blot experiments, and found that the expression of GS in U87 cells increased, while that in U251 cells decreased (Fig. 5c). We hypothesized that these differences in altered GS protein expression in the two cell lines after exogenous Gln deprivation led to the difference in their sensitivity to the loss of exogenous Gln. Data from MTT assays also showed that Gln deprivation could inhibit the activity of glioma cells.

After determining this difference in Gln metabolism between U87 and U251 cells, to determine whether the two treatments, carnosine and Gln deprivation, would have a synergistic inhibitory effect on the proliferation of U87 and U251 glioma cells, which exhibit differences in Gln metabolism, we conducted MTT assays. The results showed that 50 mM carnosine combined with Gln deprivation decreased the activity of U87 and U251 cells by 67% and 61%, respectively (48 h under hypoxia), and that this combined inhibition was stronger than that of Gln deprivation alone or carnosine alone (Fig. 5a, b). However, the expected synergistic effect was not observed in U251 cells at 72 h after they received the two treatments, indicating that carnosine could no longer further strengthen the effect of Gln, but this synergistic effect was still observed in U87 cells. We speculated that this difference is related to the different dependencies of the two cell lines on Gln. In addition, carnosine still showed an inhibitory effect on GS protein expression during Gln deprivation (Fig. 5c). The above data indicated that carnosine significantly inhibited the proliferation of glioma cells under conditions of Gln deprivation, and that this effect may be related to the inhibition of GS expression by carnosine.

Whether carnosine combined with Gln deprivation could induce cell apoptosis and decrease cell viability remained uncertain. To examine this question, we conducted flow cytometry analysis. The results showed that the proportion of apoptotic U87 and U251 cells after 48 h under normoxic conditions was significantly higher following treatment with carnosine combined with Gln compared with treatment with carnosine or Gln alone. The apoptosis rate of U87 cells treated with carnosine was 7.72%, that of the Gln-deprivation group was

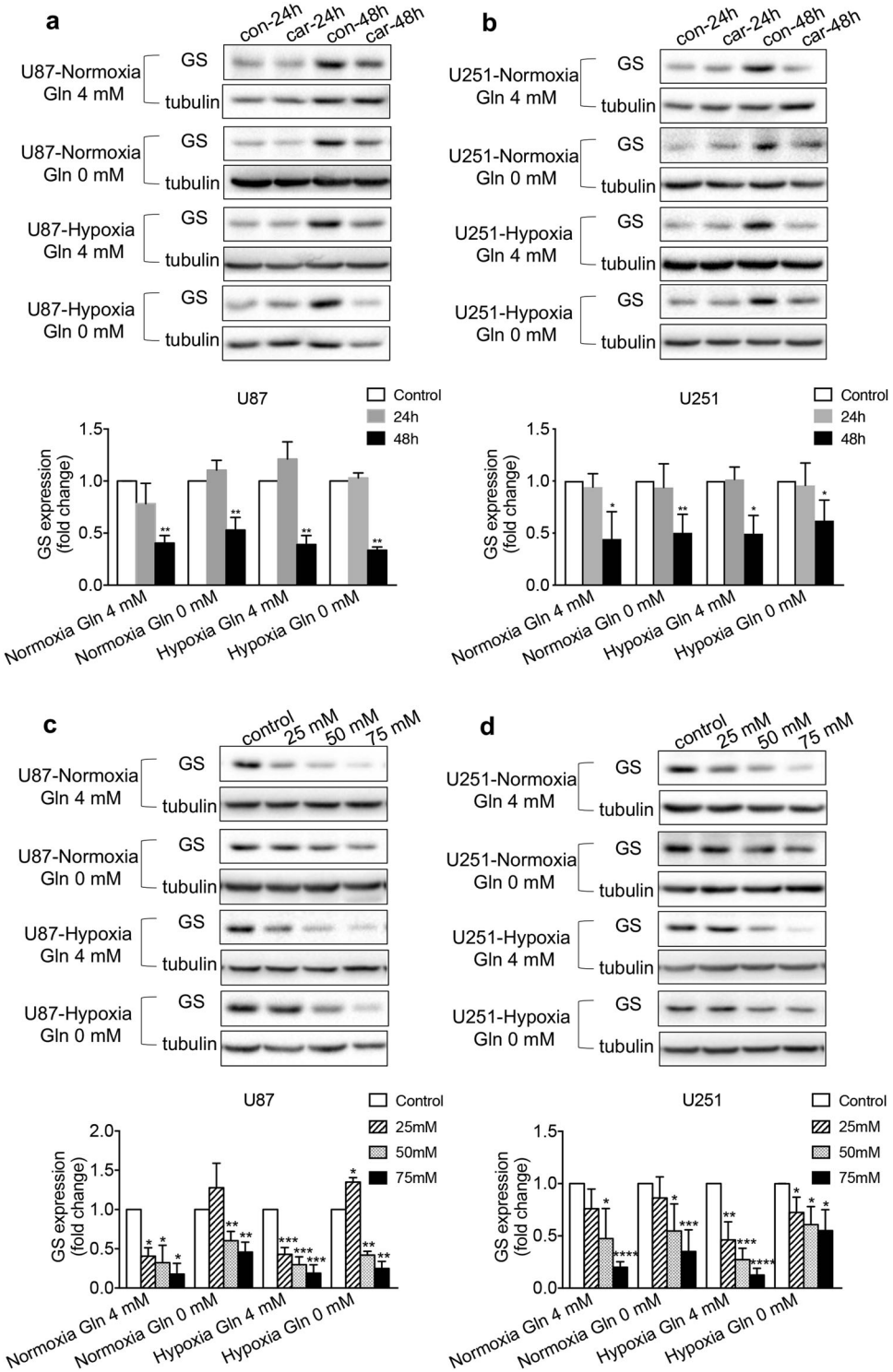

Fig. 4 Time- and concentration-dependent inhibitory effect of carnosine on GS expression in U87 and U251 cells under conditions of normoxia, hypoxia, Gln (4 mM) treatment, and Gln deprivation. Under different conditions, cells were treated with 50 mM carnosine for different durations (24 and 48 h) (**a**, **b**) or treated with different concentrations of carnosine (25, 50, and 75 mM) for 48 h (**c**, **d**). Western blot experiments were performed to detect GS levels. The results are expressed as the mean ± SD. $n \geq 3$. *$P < 0.05$, **$P < 0.01$, ***$P < 0.001$, ****$P < 0.0001$ vs. control group.

7.03%, and that of carnosine combined with Gln-deprivation group was 11.98%. The apoptosis rate of U251 cells was 8.89% in the carnosine-treatment group, 10.40% in the Gln-deprivation group, and 16.01% in carnosine combined with Gln-deprivation group (Fig. 5d).

Inhibition of the Gln metabolism pathway suppressed the proliferation, migration, and invasion of glioma cells, and carnosine treatment exerted additional inhibitory effects

To study the effect of Gln pathway inhibition on the development of human glioma cells, and determine whether the Gln pathway is

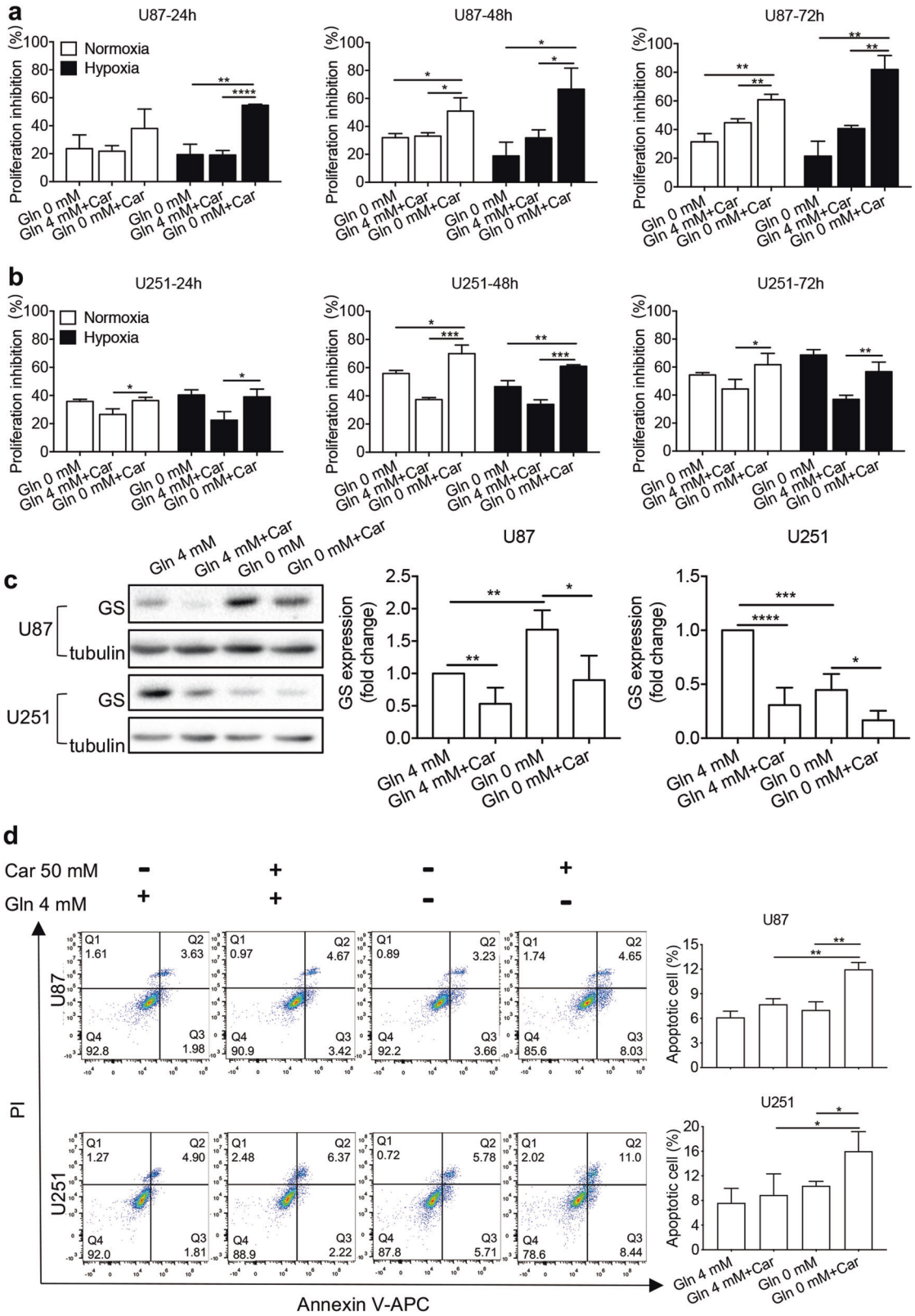

Fig. 5 Carnosine combined with Gln deprivation inhibited the growth of U87 and U251 cells and induced apoptosis. U87 cells (**a**) and U251 cells (**b**) were treated with Gln deprivation, 50 mM carnosine, or both for different time periods (24, 48, and 72 h) under normoxic and hypoxic conditions. Cell viability was measured by MTT assay, and the proliferation inhibition rate was calculated as (absorbance of the control group−absorbance of the treatment group)/absorbance of the control group × 100%. **c** Under normoxia, cells were deprived of Gln or treated with 50 mM carnosine for 48 h, after which the GS level was detected by Western blot assay. **d** Under normoxia, cells were deprived of Gln or treated with 50 mM carnosine for 48 h, after which flow cytometry was used to detect the apoptosis level. Mean ± SD. $n = 3–5$. *$P < 0.05$, **$P < 0.01$, ***$P < 0.001$, ****$P < 0.0001$ vs. 0 mM Gln treatment, 4 mM Gln + Car treatment, 4 mM Gln treatment, or 0 mM Gln treatment.

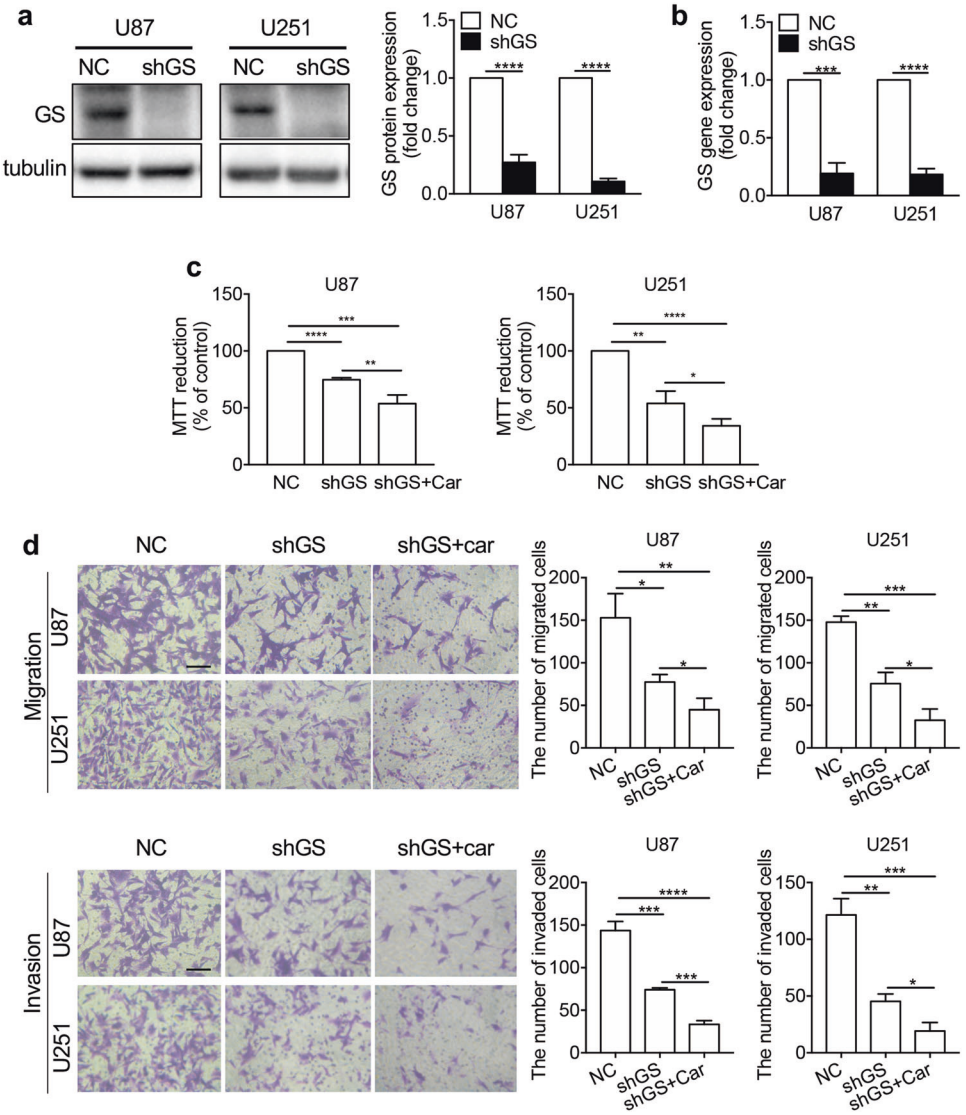

Fig. 6 The inhibitory effect of carnosine on the proliferation and metastasis of U87 and U251 cells was partly achieved by inhibiting Gln metabolism. A lentivirus system and puromycin selection were used to establish GS cell lines with low stable GS expression (shGS) and control cell lines (NC). Western blot experiments (**a**) were used to identify GS protein expression in the cell lines; real-time PCR (**b**) was used to identify GS transcription levels. Under conditions of exogenous Gln deprivation, shGS cells were treated with 50 mM carnosine, and cell viability was tested by MTT assays (**c**). Transwell assays (**d**) were used to detect cell migration and invasion capacity. Scale bar = 100 μm. The results are expressed as the mean ± SD. $n = 3$. *$P < 0.05$, **$P < 0.01$, ***$P < 0.001$, ****$P < 0.0001$ vs. NC or shGS group.

the only target of carnosine, we infected U87 and U251 cells with packaged GS-targeted RNA-interference lentiviral plasmids. Puromycin was used to screen stably transfected cells, and changes in GS protein and mRNA levels in stably transfected cells were verified by Western blotting and real-time PCR. The protein expression levels of GS in the shGS groups of U87 and U251 cells decreased by 72.78% ± 3.78% and 89.33% ± 0.97%, respectively, and the GS mRNA levels decreased by 80.76% ± 5.26% and 81.68% ± 2.85%, respectively, compared with those in the NC (negative control) group (Fig. 6a, b).

To verify the effect of the Gln metabolic pathway on the proliferation of U87 and U251 cells, and determine whether carnosine has multiple targets, MTT assays were carried out under conditions of exogenous Gln deprivation. The inhibition of Gln metabolism decreased cell viability. Comparison of the shGS groups and NC groups showed that U87 and U251 cell viability decreased by 25.32% ± 1.03% and 46.02% ± 6.16%, respectively. Furthermore, comparison of the shGS + Car groups and NC groups showed that U87 and U251 cell viability decreased by 46.34% ± 4.42% and 65.77% ± 3.54%, respectively (Fig. 6c). Subsequently, we performed Transwell experiments under conditions of Gln deprivation, and verified the effect of the Gln metabolic pathway on the migration and invasion of U87 and U251 cells. The number of cells that passed through the membrane was significantly lower in the shGS group than in the NC group. In the migration assay (Fig. 6d), among U87 and U251 cells, compared with the NC group, migration in the shGS group was decreased by 49.36% and 48.84%, respectively, and that in the shGS + car group was decreased by 70.63% and 77.93%, respectively. In the invasion experiment (Fig. 6d), among U87 and U251 cells, invasion of the shGS group was decreased by 48.45% and 62.66%, respectively, compared with that in the NC group, and invasion of the shGS + car group was decreased by 76.72% and 84.28%, respectively, compared with that in the NC group. The above data showed that inhibition of the Gln metabolic pathway had an inhibitory effect on the proliferation,

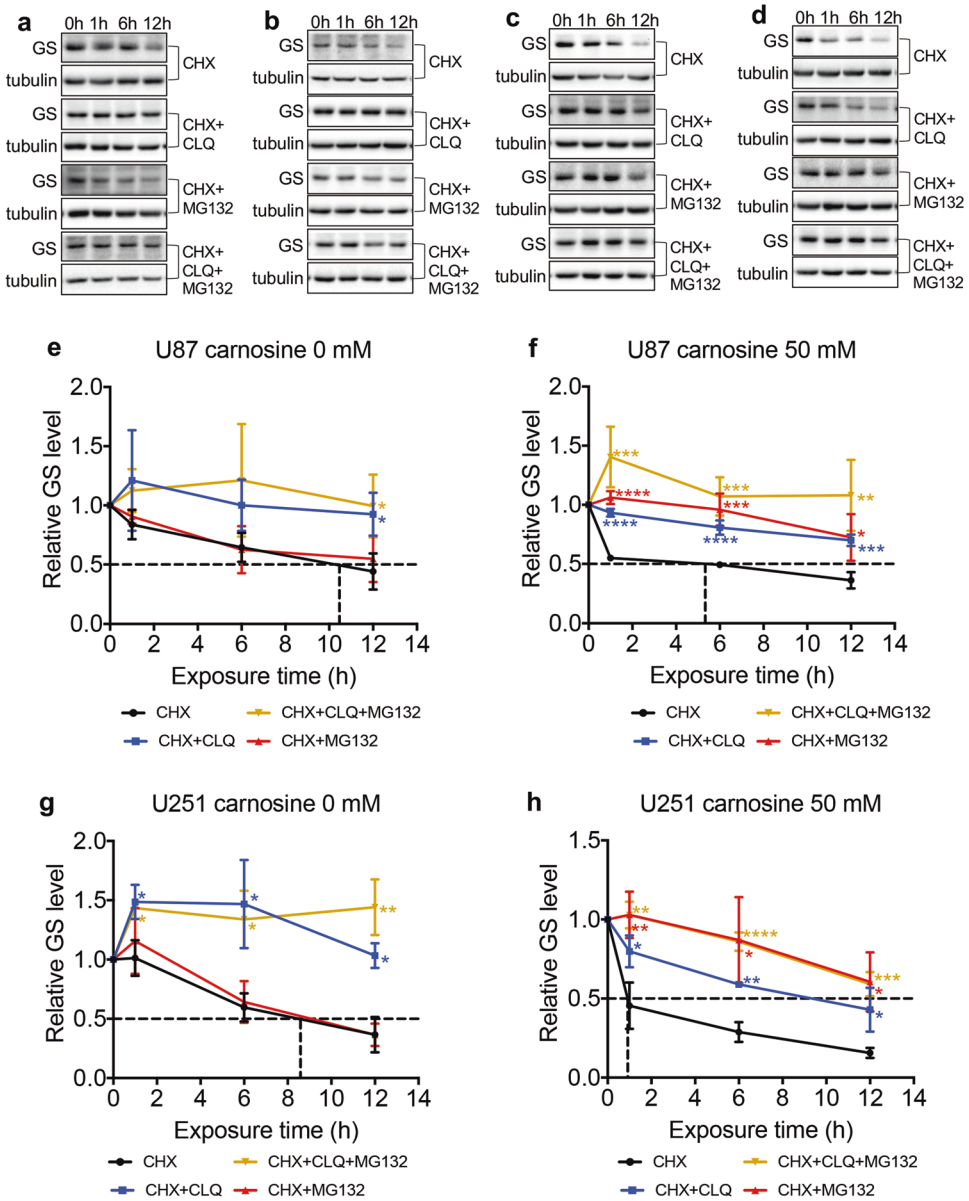

Fig. 7 Carnosine reduced the stability of the GS protein in U87 and U251 cells, shortened the half-life of the GS protein, and accelerated degradation of the GS protein by the proteasome pathway. U87 cells without carnosine treatment (**a**, **e**), U87 cells with carnosine treatment (**b**, **f**), U251 cells without carnosine treatment (**c**, **g**), and U251 cells with carnosine treatment (**d**, **h**) were cultured for up to 12 h in the presence of CHX (150 μg/mL), CHX plus the lysosome inhibitor CLQ (25 μM, CHX + CLQ), CHX plus the proteasome inhibitor MG132 (5 μM, CHX + MG132), or CHX plus MG132 and CLQ (CHX + MG132 + CLQ). Cell lysates were prepared at the indicated time points and immunoblotted with anti-GS and anti-tubulin (**a**–**d**). **e**–**h** The *X*-axis coordinate corresponding to the dashed line represents the half-life of the GS protein obtained when cells were treated with CHX alone. The results are expressed as the mean ± SD. $n \geq 3$. *$P < 0.05$, **$P < 0.01$, ***$P < 0.001$, ****$P < 0.0001$ vs. the CHX group.

migration, and invasion of U87 and U251 cells, and that the inhibitory effect of carnosine on glioma cells was partially achieved through the Gln metabolic pathway.

Carnosine accelerated the rate of GS degradation via the ubiquitin–proteasome pathway

We further sought to determine whether the carnosine-induced reduction in GS was due to enhanced degradation. To detect the half-life of GS, U87 and U251 cells were treated with CHX (150 μg/mL) alone or in combination with carnosine, to stop the synthesis of new GS. Then, we collected cell lysates at different time points after CHX treatment and immunoblotted the cell lysates with anti-GS antibody. The data showed that the half-life of GS was significantly shortened from 10.4 h and 8.5 h in control U87 and U251 cells (Fig. 7e, g), respectively, to 5.3 h and 0.9 h in carnosine-treated U87 and U251 cells, respectively (Fig. 7f, h).

Protein half-life is regulated by the proteasome and lysosome pathways. We wanted to determine which pathway was responsible for the GS degradation observed in U87 and U251 cells, and whether this pathway of GS degradation in U87 and U251 cells was altered as a result of carnosine treatment. We treated control and carnosine-exposed cells in the presence of CHX with the proteasome inhibitor MG132 (5 μM) or the lysosome inhibitor CLQ (25 μM) separately or in combination. The results showed that the control group cultured in the presence of either CHX alone or CHX combined with MG132 presented comparable levels of partial blockade of GS degradation, while U87 and U251 cells cultured in the presence of CHX combined with CLQ

demonstrated complete blockade of GS degradation (Fig. 7a, c), suggesting that GS in U87 and U251 cells was degraded mainly through the lysosome pathway rather than the proteasome pathway. In contrast, in carnosine-exposed cells, the combination of either MG132 or CLQ with CHX partially blocked GS degradation, while the combination of MG132 and CLQ with CHX completely blocked GS degradation in control cells (Fig. 7b, d), indicating that GS is degraded through both the proteasome and lysosome pathways in carnosine-exposed cells. These findings suggest that in U87 and U251 cells, carnosine likely shortened the GS half-life through accelerating the proteasomal degradation of GS.

DISCUSSION

In this study, we demonstrated the inhibitory effect of carnosine on Gln metabolism in human glioma cells under normoxic and hypoxic conditions, and the underlying mechanism of carnosine. Our principal findings are as follows: first, carnosine inhibited the proliferation, migration, and invasion of U87 and U251 cells, but the inhibitory effects of carnosine under normoxic and hypoxic conditions did not significantly differ. Second, the inhibitory effect of carnosine on U87 and U251 cells was partly achieved by inhibiting the Gln metabolism pathway, which plays an important role in the regulation of human glioma cell proliferation, migration, and invasion. Third, carnosine reduced the expression of GS in U87 and U251 cells by promoting the degradation of GS through the proteasome pathway, shortening the protein half-life, and reducing its stability. Therefore, carnosine should be considered among many other compounds that target tumor metabolism, one of the key hallmarks of tumors, in various stages of drug development.

Currently, the mechanism of these carnosine-mediated effects has not yet been clarified, and whether the inhibitory effects of carnosine under normoxia and hypoxia are different is not known. In the current study, we detected the viability, colony-formation capacity, and apoptosis of U87 and U251 cells treated with 50 mM carnosine under normoxic and hypoxic conditions. We found that carnosine treatment reduced the mitochondrial activity of glioma cells in a time- and concentration-dependent manner, and that there was no significant difference in this inhibitory effect between normoxic and hypoxic conditions. The above results were further proven by the colony-formation assay. Studies have demonstrated the occurrence of relatively high amounts of carnosine (0.01–0.2 μg/g) in the brains of rodents [27]. However, in the brain, carnosine is mainly distributed in glial cells, particularly astrocytes. Thus, the concentration of carnosine in astrocytes is much higher than 0.01–0.2 μg/g. In addition, in some other studies on carnosine and tumors, the concentration of carnosine was found to be almost 50 mM [21, 28]. We used such a high level of carnosine because of the presence of carnosine hydrolase in the serum, which is also an obstacle to the clinical use of carnosine. We learned from an article that serum carnosine hydrolase has been modeled, and that it is possible to design specific drugs to inhibit its effect [29]. In addition, some modifications have been made to the molecular structure of carnosine so that it cannot be hydrolyzed by related enzymes, making carnosine clinically valuable. Therefore, for the present study, we selected carnosine at a concentration of 50 mM to investigate the antitumor effects of carnosine on glioma cells cultured under normoxic and hypoxic conditions. However, by flow cytometry analysis, we found that 50 mM carnosine did not affect the apoptosis level of glioma cells.

Our results also demonstrated that hypoxia did not induce apoptosis in either cell line. By analyzing the viability and colony-forming ability of U87 and U251 cells under normoxic and hypoxic conditions, we found that short-term (72 h) hypoxia treatment decreased U87 cell viability, while long-term (14 days) hypoxia treatment enhanced U87 and U251 cell colony-forming ability (Supplementary Fig. 2). We speculate that long-term hypoxia treatment led to cell adaptability and increased the malignant proliferation capacity. Short-term hypoxia may lead to stress injury in cells, resulting in a certain degree of decreased cell viability, migration, and invasion, but carnosine still showed a strong inhibitory effect, regardless of this decline, and there was no difference in the inhibitory effect of carnosine between cell lines. The results suggest that carnosine can target both the glycolysis and mitochondrial oxidative metabolism pathways to inhibit the proliferation, migration, and invasion of glioma cells. Hypoxia, one of the characteristics of most solid tumors, can promote tumor progression and enhance resistance to treatment, constituting a great challenge to treatment [30]. With the continuous proliferation of glioma cells, the oxygen supply inside the tumor is insufficient, showing a state of hypoxia, while the relatively external glioma cells can obtain sufficient oxygen and energy materials. Glioma tumor growth can be promoted through glycolysis and mitochondrial aerobic respiration. Our results showed that carnosine had a significant inhibitory effect on glioma cells under hypoxic conditions, and did not show resistance to a change in oxygen concentration in the tumor microenvironment. Wound-healing and Transwell assays also showed that carnosine could inhibit the migration and invasion of glioma cells, and the inhibitory effects of carnosine under normoxic and hypoxic conditions were similar. The inhibitory effect of carnosine on the metastasis of tumor cells may be related to its inhibition of nonenzymatic glycosylation. Glycosylation is a form of synthetic protein modification with physiological and pathological functions. In the process of metastasis, glycosylation on the surface of tumor cells is related to the malignant enhancement of tumors [31]. However, the exact mechanism by which carnosine inhibits glioma cell metastasis needs further study.

Gln is a nitrogen and carbon source with which cells synthesize nucleotides and amino acids [32]. It plays a variety of metabolic and nonmetabolic roles, and is essential for glioma growth. In recent years, most studies on Gln metabolism and tumors have focused on Gln catabolism, glutaminase (GLS), and glutamine transporters [33–35]. However, some researchers have found that inhibition of Gln decomposition does not affect glioma cell proliferation [14]. Only a few researchers have focused on the relationship between Gln anabolism and tumors. In sarcomas, GS mediates the proliferation of Gln-deprived pediatric sarcomas [36]; Anna Rosati and other researchers found that no/low GS expression was significantly associated with prolonged survival in glioma patients [25]. In the present study, we found that carnosine inhibited GS expression at the translation level. Hypoxia treatment led to a decrease in the protein expression of GS in glioma cells, but had little effect on the GS transcription level. HIF-1α and GS expression have been shown to be correlated [37]. We speculated that the downregulation of GS protein expression in glioma cells under hypoxia may be related to HIF-1α, but the specific mechanism needs further study. Our study showed that regardless of the oxygen conditions or the presence/absence of Gln, when carnosine at different concentrations was used to treat glioma cells for different time intervals, the expression level of GS decreased in a concentration- and time-dependent manner, which indicated that the expression of GS was indeed inhibited by carnosine. Then, we deprived glioma cells of Gln and treated them with carnosine for different time periods. The U87 and U251 cells were inhibited to different degrees by Gln deprivation, which was consistent with some studies on the Gln dependence of cancer cells [38, 39]. Interestingly, U87 cells were more tolerant to Gln deprivation, while U251 cells were more sensitive, suggesting considerable heterogeneity among gliomas, similar to a study in which tissue microarray (TMA) analysis was used to detect GS expression in human glioma ($n = 209$ patients). The authors found

that the expression of GS varied greatly among different tumors, ranging from negative expression in neuronal tumors (25% of patients) to high expression in astrocyte tumors (15% of patients) [14]. After an in-depth study of this interesting phenomenon, we found that GS expression in U87 cells increased, while that in U251 cells decreased, after Gln deprivation, which may explain the difference in sensitivity to Gln deprivation between the two glioma cell lines. Moreover, our results suggested that the combined effect of carnosine and Gln deprivation may significantly inhibit cell viability by inducing apoptosis, which may be related to changes in the expression levels of the apoptosis-related factors Bcl-2, Bax, caspase, and NF-κB [40].

To clarify the effect of the Gln metabolic pathway on the malignant phenotype of human glioma cells, we performed MTT and Transwell experiments in cells expressing low levels of GS under conditions of exogenous Gln deprivation. The results showed that inhibition of the Gln metabolic pathway could significantly inhibit glioma cell proliferation and metastasis. In this context, carnosine treatment still had a significant inhibitory effect, which showed that the inhibitory effect of carnosine on glioma cells was partially realized through the Gln metabolism pathway. This is the first study to show that the mechanism of carnosine's antitumor activity is related to Gln metabolism, which is consistent with the notion that the antitumor effect of carnosine involves multiple targets [26].

In our study, carnosine changed GS expression at only the protein level in glioma cells, but did not affect the RNA expression level of GS. To further study the pathway by which carnosine downregulated GS expression, we first treated glioma cells with CHX and then measured changes in the half-life of the GS protein in glioma cells after carnosine treatment. The half-life of the GS protein in glioma cells was decreased by carnosine treatment, as shown in Fig. 7. At present, evidence has shown two major proteolytic pathways, proteasome-mediated degradation, and lysosome-mediated proteolysis, both of which are conserved from yeasts to humans [41]. In this study, we found that the GS protein was mainly degraded by the lysosomal pathway in glioma cells without carnosine treatment, and GS degradation level by the proteasome pathway was significantly increased after carnosine treatment. As the most important method of protein degradation in cells, the ubiquitin–proteasome system plays an important role in regulating tumor growth, so it has become the target of cancer treatment. Interestingly, given the many examples of ubiquitin ligase dysregulation in brain tumors, inhibition of the proteasome may not be an appropriate molecular target to halt tumorigenesis. In contrast, activation or enhancement of the degradation of key proteasome substrates may be a more reasonable strategy [42]. Although we found that carnosine could affect the malignant phenotype of glioblastoma cells through the proteasome pathway, the in-depth mechanism still needs to be verified. Here, we speculate that carnosine promotes the expression of ubiquitinated proteins, activates the proteasome, or increases proteasome component expression, which may change GS protein levels in glioma cells.

In conclusion, this study showed that carnosine could significantly inhibit the proliferation, migration, and invasion of U87 and U251 cells under normoxic and hypoxic conditions, and that the inhibitory effect of carnosine on U87 and U251 cells did not significantly differ under normoxic and hypoxic conditions. The Gln metabolic pathway plays an important role in the growth and metastasis of glioma cells, and this study is the first to confirm that the inhibitory effect of carnosine on glioma cells was exerted partly through the Gln metabolic pathway. Carnosine may promote GS protein degradation through the proteasome pathway. Our findings demonstrate that carnosine is a potential drug targeting tumor metabolism that can inhibit the proliferation and metastasis of human glioma cells.

ACKNOWLEDGEMENTS

This work was supported by Zhejiang Provincial Scientific Research Foundations (LY19H090010), Wenzhou City Science and Technology Project (Y20170014), and Key Discipline of Zhejiang Province in Medical Technology (First Class, Category A).

AUTHOR CONTRIBUTIONS

YS and JXL conceived and designed the experiments; YJF and YS wrote the paper; YJF, MW, HNC, and TTW performed experiments and analyzed the data.

ADDITIONAL INFORMATION

The online version of this article (https://doi.org/10.1038/s41401-020-0488-1) contains supplementary material, which is available to authorized users.

Competing interests: The authors declare no competing interests.

REFERENCES

1. Lapointe S, Perry A, Butowski NA. Primary brain tumours in adults. Lancet. 2018;392:432–46.
2. Ostrom QT, Gittleman H, Truitt G, Boscia A, Kruchko C, Barnholtz-Sloan JS. CBTRUS statistical report: primary brain and other central nervous system tumors diagnosed in the United States in 2011-2015. Neuro Oncol. 2018;20:iv1–iv86.
3. Cheng F, Guo D. MET in glioma: signaling pathways and targeted therapies. J Exp Clin Cancer Res. 2019;38:270.
4. Tomiyama A, Ichimura K. Signal transduction pathways and resistance to targeted therapies in glioma. Semin Cancer Biol. 2019;58:118–29.
5. Bao S, Wu Q, McLendon RE, Hao Y, Shi Q, Hjelmeland AB, et al. Glioma stem cells promote radioresistance by preferential activation of the DNA damage response. Nature. 2006;444:756–60.
6. Cheng L, Huang Z, Zhou W, Wu Q, Donnola S, Liu JK, et al. Glioblastoma stem cells generate vascular pericytes to support vessel function and tumor growth. Cell. 2013;153:139–52.
7. Xue H, Yuan G, Guo X, Liu Q, Zhang J, Gao X, et al. A novel tumor-promoting mechanism of IL6 and the therapeutic efficacy of tocilizumab: Hypoxia-induced IL6 is a potent autophagy initiator in glioblastoma via the p-STAT3-MIR155-3p-CREBRF pathway. Autophagy. 2016;12:1129–52.
8. Brat DJ, Castellano-Sanchez AA, Hunter SB, Pecot M, Cohen C, Hammond EH, et al. Pseudopalisades in glioblastoma are hypoxic, express extracellular matrix proteases, and are formed by an actively migrating cell population. Cancer Res. 2004;64:920–7.
9. Zong WX, Rabinowitz JD, White E. Mitochondria and cancer. Mol Cell. 2016;61:667–76.
10. Shen Y, Yang J, Li J, Shi X, Ouyang L, Tian Y, et al. Carnosine inhibits the proliferation of human gastric cancer SGC-7901 cells through both of the mitochondrial respiration and glycolysis pathways. PLoS ONE. 2014;9:e104632.
11. Diers AR, Broniowska KA, Chang CF, Hogg N. Pyruvate fuels mitochondrial respiration and proliferation of breast cancer cells: effect of monocarboxylate transporter inhibition. Biochem J. 2012;444:561–71.
12. Eagle H, Oyama VI, Levy M, Horton CL, Fleischman R. The growth response of mammalian cells in tissue culture to *L*-glutamine and *L*-glutamic acid. J Biol Chem. 1956;218:607–16.
13. Marin-Valencia I, Yang C, Mashimo T, Cho S, Baek H, Yang XL, et al. Analysis of tumor metabolism reveals mitochondrial glucose oxidation in genetically diverse human glioblastomas in the mouse brain in vivo. Cell Metab. 2012;15:827–37.
14. Tardito S, Oudin A, Ahmed SU, Fack F, Keunen O, Zheng L, et al. Glutamine synthetase activity fuels nucleotide biosynthesis and supports growth of glutamine-restricted glioblastoma. Nat Cell Biol. 2015;17:1556–68.
15. Caruso G, Caraci F, Jolivet RB. Pivotal role of carnosine in the modulation of brain cells activity: multimodal mechanism of action and therapeutic potential in neurodegenerative disorders. Prog Neurobiol. 2019;175:35–53.
16. Sarrami F, Yu LJ, Karton A. Computational design of bio-inspired carnosine-based HOBr antioxidants. J Comput Aided Mol Des. 2017;31:905–13.
17. Miceli V, Pampalone M, Frazziano G, Grasso G, Rizzarelli E, Ricordi C, et al. Carnosine protects pancreatic beta cells and islets against oxidative stress damage. Mol Cell Endocrinol. 2018;474:105–18.
18. Seidler NW, Yeargans GS, Morgan TG. Carnosine disaggregates glycated alpha-crystallin: an in vitro study. Arch Biochem Biophys. 2004;427:110–5.
19. Artioli GG, Sale C, Jones RL. Carnosine in health and disease. Eur J Sport Sci. 2019;19:30–9.

20. Ditte Z, Ditte P, Labudova M, Simko V, Iuliano F, Zatovicova M, et al. Carnosine inhibits carbonic anhydrase IX-mediated extracellular acidosis and suppresses growth of HeLa tumor xenografts. BMC Cancer. 2014;14:358.
21. Oppermann H, Faust H, Yamanishi U, Meixensberger J, Gaunitz F. Carnosine inhibits glioblastoma growth independent from PI3K/Akt/mTOR signaling. PLoS One. 2019;14:e0218972.
22. Cheng JY, Yang JB, Liu Y, Xu M, Huang YY, Zhang JJ, et al. Profiling and targeting of cellular mitochondrial bioenergetics: inhibition of human gastric cancer cell growth by carnosine. Acta Pharmacol Sin. 2019;40:938–48.
23. Cao P, Zhang J, Huang Y, Fang Y, Lyu J, Shen Y. The age-related changes and differences in energy metabolism and glutamate-glutamine recycling in the d-gal-induced and naturally occurring senescent astrocytes in vitro. Exp Gerontol. 2019;118:9–18.
24. Holliday R, McFarland GA. A role for carnosine in cellular maintenance. Biochem (Mosc). 2000;65:843–8.
25. Rosati A, Poliani PL, Todeschini A, Cominelli M, Medicina D, Cenzato M, et al. Glutamine synthetase expression as a valuable marker of epilepsy and longer survival in newly diagnosed glioblastoma multiforme. Neuro Oncol. 2013;15:618–25.
26. Hipkiss AR, Gaunitz F. Inhibition of tumour cell growth by carnosine: some possible mechanisms. Amino Acids. 2014;46:327–37.
27. Pisano JJ, Wilson JD, Cohen L, Abraham D, Udenfriend S. Isolation of gamma-aminobutyrylhistidine (homocarnosine) from brain. J Biol Chem. 1961;236:499–502.
28. Renner C, Asperger A, Seyffarth A, Meixensberger J, Gebhardt R, Gaunitz F. Carnosine inhibits ATP production in cells from malignant glioma. Neurol Res. 2010;32:101–5.
29. Qiu J, Hauske SJ, Zhang S, Rodriguez-Nino A, Albrecht T, Pastene DO, et al. Identification and characterisation of carnostatine (SAN9812), a potent and selective carnosinase (CN1) inhibitor with in vivo activity. Amino Acids. 2019;51:7–16.
30. Cavazos DA, Brenner AJ. Hypoxia in astrocytic tumors and implications for therapy. Neurobiol Dis. 2016;85:227–33.
31. Hauselmann I, Borsig L. Altered tumor-cell glycosylation promotes metastasis. Front Oncol. 2014;4:28. https://doi.org/10.3389/fonc.2014.00028.
32. DeBerardinis RJ, Mancuso A, Daikhin E, Nissim I, Yudkoff M, Wehrli S, et al. Beyond aerobic glycolysis: transformed cells can engage in glutamine metabolism that exceeds the requirement for protein and nucleotide synthesis. Proc Natl Acad Sci USA. 2007;104:19345–50.
33. Yang L, Venneti S, Nagrath D. Glutaminolysis: A Hallmark of Cancer Metabolism. Annu Rev Biomed Eng. 2017;19:163–94.
34. Altman BJ, Stine ZE, Dang CV. From Krebs to clinic: glutamine metabolism to cancer therapy. Nat Rev Cancer. 2016;16:619–34.
35. Yoo HC, Park SJ, Nam M, Kang J, Kim K, Yeo JH, et al. A Variant of SLC1A5 Is a mitochondrial glutamine transporter for metabolic reprogramming in cancer cells. Cell Metab. 2020;31:267–83. e12
36. Issaq SH, Mendoza A, Fox SD, Helman LJ. Glutamine synthetase is necessary for sarcoma adaptation to glutamine deprivation and tumor growth. Oncogenesis. 2019;8:20. https://doi.org/10.1038/s41389-019-0129-z.
37. Kitajima S, Lee KL, Hikasa H, Sun W, Huang RY, Yang H, et al. Hypoxia-inducible factor-1alpha promotes cell survival during ammonia stress response in ovarian cancer stem-like cells. Oncotarget. 2017;8:114481–94.
38. Vanhove K, Derveaux E, Graulus GJ, Mesotten L, Thomeer M, Noben JP, et al. Glutamine addiction and therapeutic strategies in lung cancer. Int J Mol Sci. 2019;20:252.
39. Marquez J, Alonso FJ, Mates JM, Segura JA, Martin-Rufian M, Campos-Sandoval JA. Glutamine addiction in gliomas. Neurochem Res. 2017;42:1735–46.
40. Fulda S. Cell death-based treatment of glioblastoma. Cell Death Dis. 2018;9:121. https://doi.org/10.1038/s41419-017-0021-8.
41. Ciechanover A. Intracellular protein degradation: from a vague idea thru the lysosome and the ubiquitin-proteasome system and onto human diseases and drug targeting. Best Pr Res Clin Haematol. 2017;30:341–55.
42. Zaky W, Manton C, Miller CP, Khatua S, Gopalakrishnan V, Chandra J. The ubiquitin-proteasome pathway in adult and pediatric brain tumors: biological insights and therapeutic opportunities. Cancer Metastasis Rev. 2017;36:617–33.